

# Efficient Field Computation Based on $N$ -Port Methods

Franz Schlagenhauer

**Abstract** – Radiating structures with distributed parameters, such as TEM waveguides or strip-lines, are considered as linear  $N$ -port networks and correlations between port currents and field strength values are calculated. Knowing the  $S$ -parameters for all accessible ports the port currents can be re-calculated for other source and load scenarios. Field strength values are then obtained as a linear combination of contributions due to the individual port currents. The effect of changing load and source parameters on fields can be investigated in a very efficient way without repeating full wave field simulations.

**Keywords** –  $N$ -Port models, electric field, magnetic fields.

## I. INTRODUCTION

Linear electrical networks are often analyzed by describing their behavior as  $N$ -ports; voltages and currents at a (small) number of accessible terminal pairs are determined as a function of an  $N$ -port matrix and the sources and terminations at all ports [1, 2]. Port currents  $[I_p]$  can e.g. be calculated in terms of an impedance matrix  $[Z]$ , port terminations  $[Z_{Term}]$ , and voltage sources  $[V_s]$ . Equation (1) represents then a linear system as shown in Figure 1:

$$[I_p] = [Z + Z_{Term}]^{-1} \cdot [V_s]. \quad (1)$$

$[Z]$  can be computed analytically or numerically for lumped element networks. A consideration as  $N$ -port is also possible for systems with distributed parameters, e.g. coupled transmission lines, or for any linear system such as coupled antenna arrangements [3, 4]. In the latter case numerical approaches are usually necessary to find  $[Z]$ . A full-wave field solver may be used to determine open port voltages  $V_{ij}$  (voltage on port  $i$  while exciting port  $j$ ) and the feeding currents  $I_j$  for each respective port:

$$Z_{ij} = \frac{V_{ij}}{I_j}. \quad (2)$$

If, during the field simulations while exciting each port individually with all non-excited ports being open (i.e. the respective port currents are zero), the electric and/or magnetic field strength  $F_j$  at an arbitrary observation point is also calculated, then coefficients  $\tilde{a}_j$ , relating the feeding port current  $I_j$  at port  $j$  and the field strength at that point can also be determined:

$$\tilde{a}_j = \frac{\tilde{F}_j}{I_j}. \quad (3)$$

When changing the excitation or termination of the  $N$ -port, new port currents  $I_{j-new}$  can be calculated using (1) and the new field strength be obtained as a linear combination of weighted contributions from all new port currents:

$$\tilde{F} = \sum_{j=1}^N \tilde{a}_j I_{j-new}. \quad (4)$$

More precisely, the field strength  $F_j$  is due to a linear combination of currents on each patch or segment of the simulation model, and these currents are themselves a linear combination of all port currents. Figure 2 illustrates this.

$$\tilde{F} = \sum_{j=1}^M \left( \tilde{f}_j \sum_{i=1}^N (p_{ij} I_i) \right) = \sum_{j=1}^M \sum_{i=1}^N (\tilde{f}_j p_{ij} I_i) = \sum_{i=1}^N (\tilde{a}_i I_i) \quad (5)$$

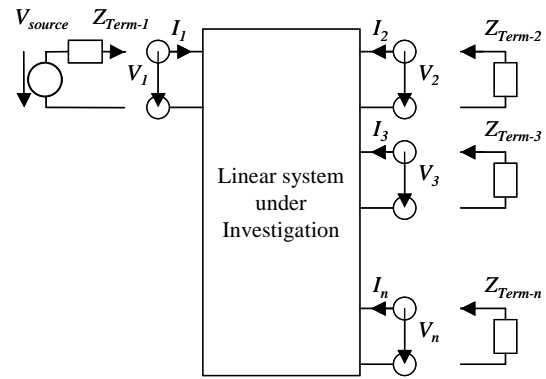


Figure 1: Linear system as  $N$ -port

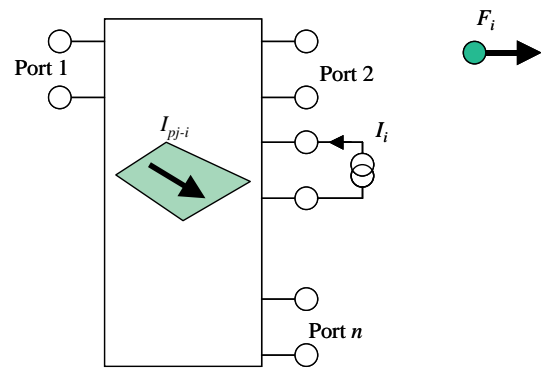


Figure 2: Field strength  $F_i$  due to port current  $I_i$

In equation (5)  $M$  stands for the number of patch and/or segment currents, and  $N$  stands for the number of accessible ports, i.e. those locations where source and load modifications are possible. In a typical Method-of-Moment model  $M$  will be in the order of several thousand, while  $N$

<sup>1</sup>The University of Western Australia, Western Australian Telecommunications Research Institute (WATRI), 39 Fairway, Nedlands WA 6907 Australia, franz-s@watri.org.au

will typically be a single digit number. Thus, not only the computation of new port currents, according to (1), where the inversion of an  $N \times N$  matrix is involved, but also the update of field strength values according to (5) is not demanding on CPU performance.

The procedure can be implemented without too much problems using software tools such as Matlab [5].

## II. TWO-PORT STRIP-LINE STRUCTURE

The method described in section I is now applied to the model of a strip-line, shown in Figure 3. The field simulation is done with a Method-of-Moment based software package [6].

First, the input impedance of the structure is used for verification of the model. The results for the base model shown in Figure 4 are not quite satisfactory. The impedance value for the 50  $\Omega$ -termination shows a good agreement only for low frequencies; the resonance frequencies differ, and the impedance magnitudes at higher frequencies are also different. For the open termination also the impedance magnitude at low frequencies is slightly different.

The end sections of the strip-line in the physical and the simulation model are shown in detail in the two inserts in Figure 4. This part of the structure has been oversimplified, and deserves more consideration. The N-connector at both ends is investigated in more detail. Measurements with a network analyzer reveal that equivalent elements are 2.7 nH when short circuited, and 1.6 pF when open. From these results the transmission line characteristics for the connector can be calculated as:

$$Z_0 = \sqrt{\frac{L'}{C'}} = \sqrt{\frac{L}{C}} = \sqrt{\frac{2.7nH}{1.6pF}} \approx 41\Omega; \quad (6)$$

$$\tau = \sqrt{LC} = \sqrt{2.7nH \times 1.6pF} \approx 66ps. \quad (7)$$

With this more sophisticated model the input impedance of the structure is calculated for exactly the same location where it is measured, i.e. at the end of the N-connector which in turn is then terminated with the basic model of the strip-line. The input impedance from the simulation is therefore

$$Z_{input} = Z_0 \frac{Z_{in} + jZ_0 \tan \beta l}{Z_0 + jZ_{in} \tan \beta l} \quad (\beta l = \omega \tau). \quad (8)$$

The input impedance  $Z_{in}$  in (8) is the impedance at the beginning of the basic strip-line when terminated with the appropriated load at its end, i.e. [2]

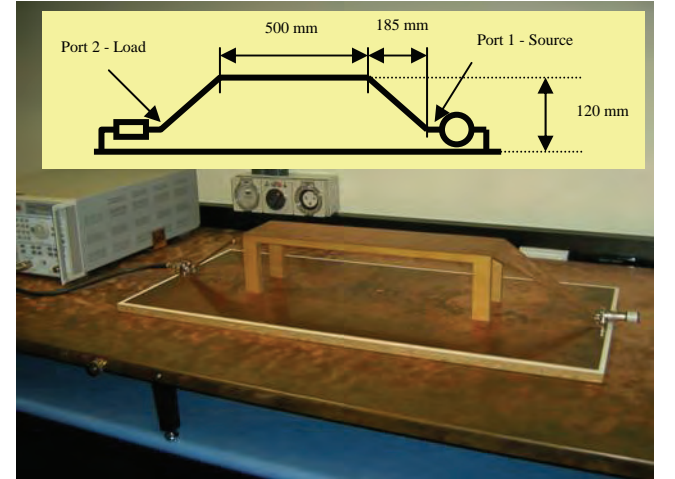
$$Z_{in} = Z_{11} - \frac{Z_{12}Z_{21}}{Z_{22} + Z_{Load}}. \quad (9)$$

$Z_{11}$ ,  $Z_{12}$ ,  $Z_{21}$  and  $Z_{22}$  are the impedance matrix elements obtained from the Method-of-Moment simulation of the basic strip-line model. The last step is now to calculate the load impedance  $Z_{Load}$  for the strip-line. This is again done by using equation (8), but now  $Z_{in}$  is replaced by the

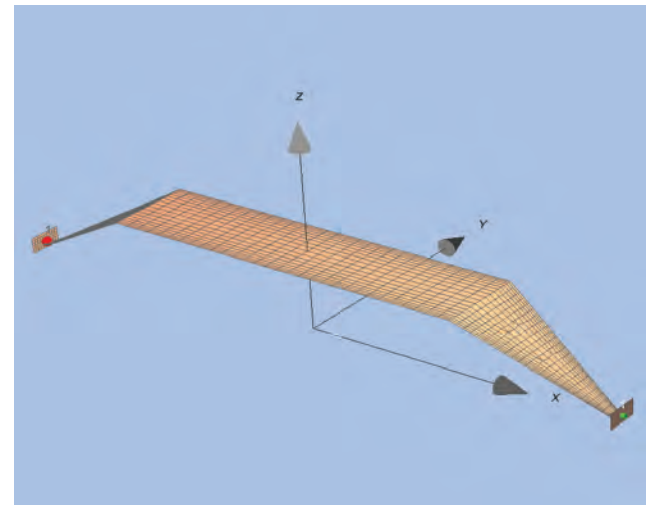
appropriate termination, e.g.  $Z_{in} \rightarrow \infty$  (open),  $Z_{in} = 50 \Omega$  or  $Z_{in} = 0$  (short circuit).

The results for the input impedance after this refinement are shown in Figure 5.  $Z_{11}$  is the input impedance of the basic strip-line model (the same as in Figure 4); when the load connector is taken into account ( $Z_{in}$ ) a slight improvement can be noted for the resonance frequency; after taking into account also the connector at the source end ( $Z_{input}$ ) a further improvement for the resonance frequencies and for the magnitude occurs. The agreement for the improved model is quite good, and this improved model is now used to calculate the field strength at one observation point for different termination scenarios.

The field strength at the centre of the strip-line, close to the ground plane is measured with a short monopole antenna, while the strip-line is excited with the network analyzer, i.e. with a voltage source with 50  $\Omega$  internal impedance, and terminated as: open, 50  $\Omega$  and short circuited. In each case, the agreement between measurements (dashed curves) and simulations (solid curves) in Figure 6 is satisfactorily.



(a) Strip-line with essential dimensions



(b) Method-of-Moment simulation model

Figure 3: Strip-line – physical structure and basic simulation model:

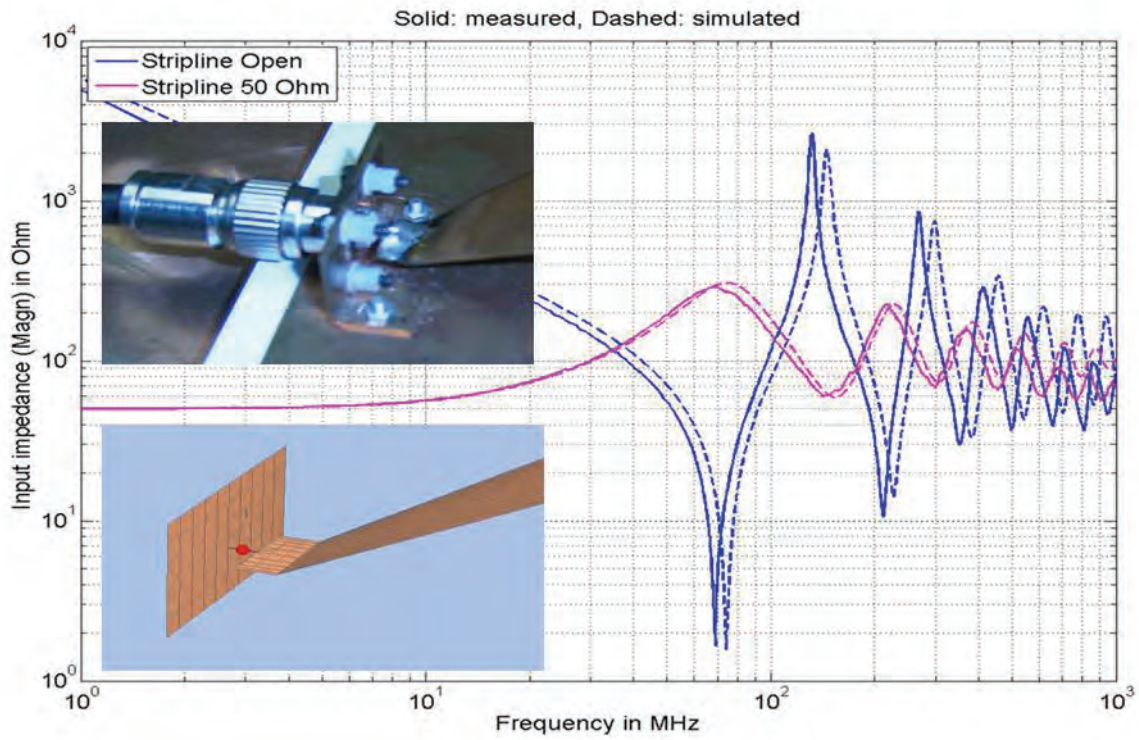


Figure 4: Input impedance – base model

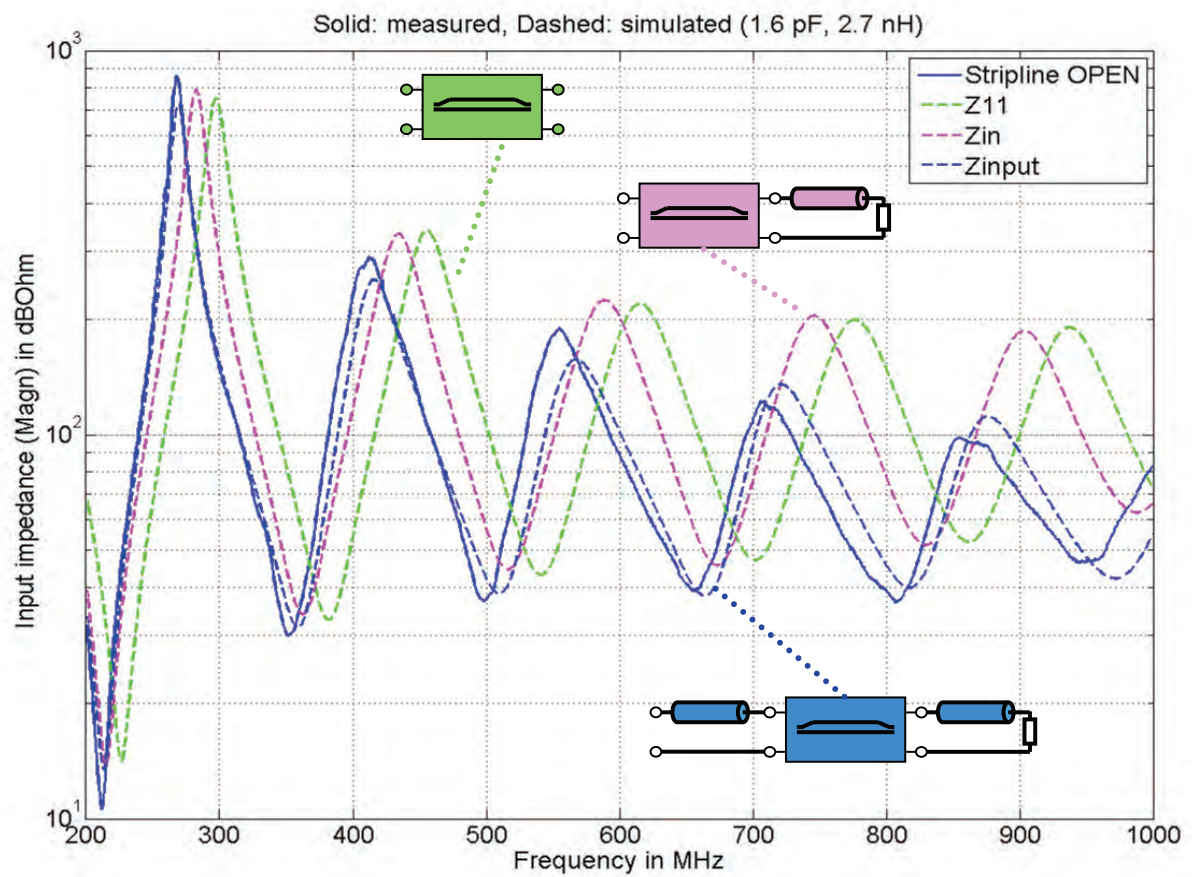


Figure 5: Input impedance – detailed modeling of terminations



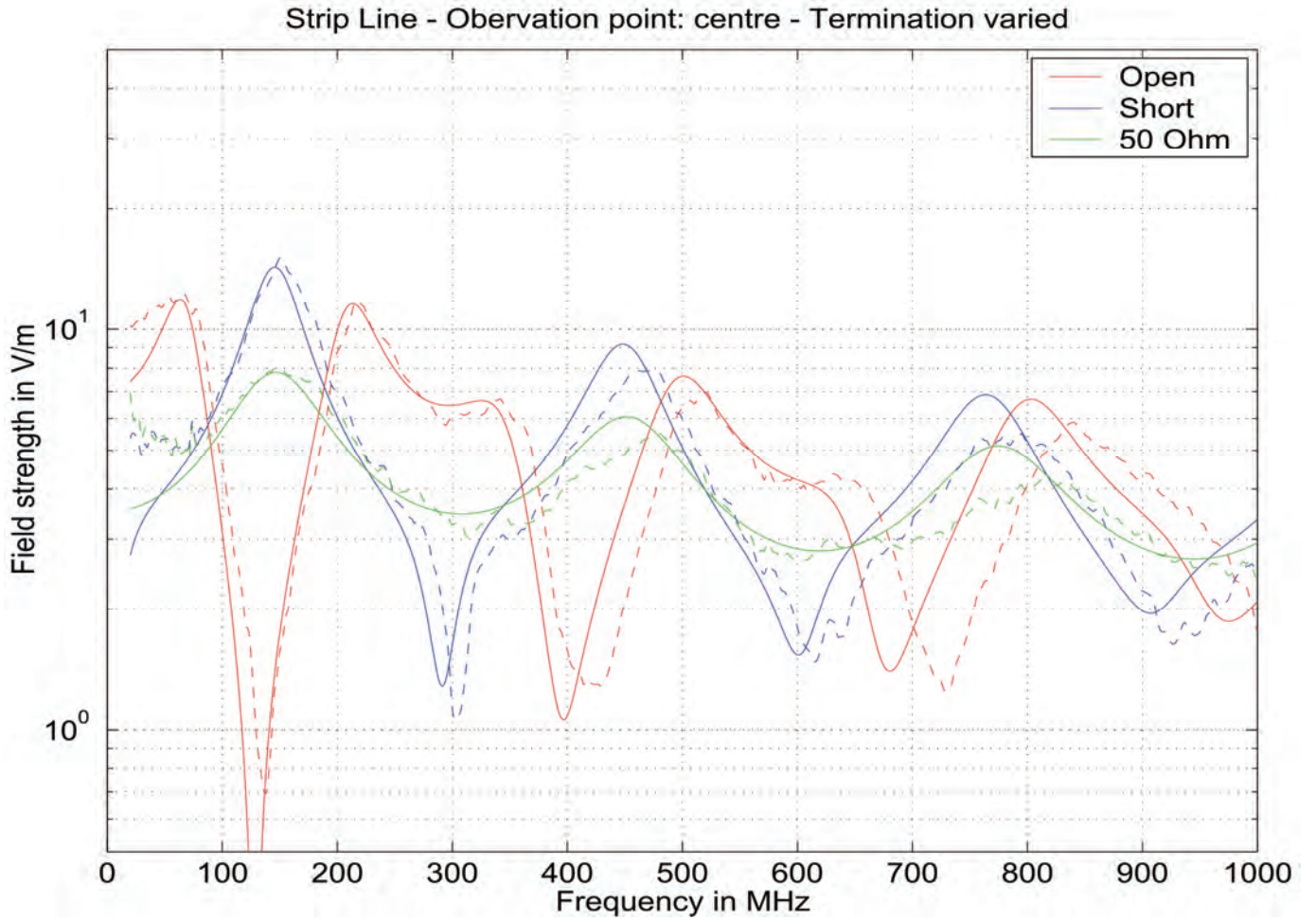


Figure 6: Field strength comparison for varied strip-line termination

### III. TEM WAVEGUIDE WITH FOUR ACCESSIBLE PORTS

The next example looks at a TEM-wave guide with four accessible ports, shown in Figure 7. Two ports are connected at either side of the septum and two ports connect the septum with the upper part of the cell for dampening cavity resonances. Septum and shell are assumed as perfect conductors [7, 8].

In initial field simulations the  $N$ -port impedance matrix and field coefficients  $a_i$  are calculated, and the electric field at one observation point (0.2m/0.2m/0.2m) is computed for a load of 50  $\Omega$  at port 2 (end of the septum). Figure 8 compares the three field components obtained by the  $N$ -port method as described in section I of this paper (solid curves), and by direct simulations (dashed curves). There is a good agreement for the dominant  $z$ -component, except for some mysterious resonances; the agreement for the other components,  $x$ - and  $y$ -, are also quite good, but again show some resonances that don't appear in the direct solution. The insert in Figure 8 shows the resonance around 33 MHz in more detail.

Figure 9 shows the maximum field strength at the same

observation point for a variation of the loads at ports 3 and 4 and for a reduced frequency range. The same occurrence of false resonances can be noted.

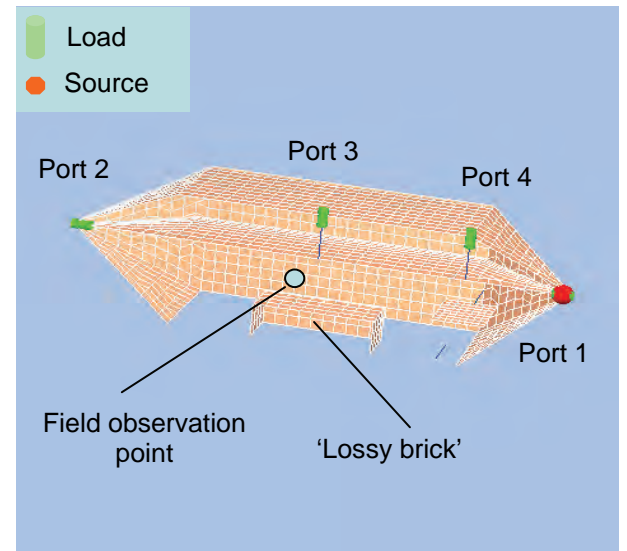


Figure 7: Four-port TEM wave guide

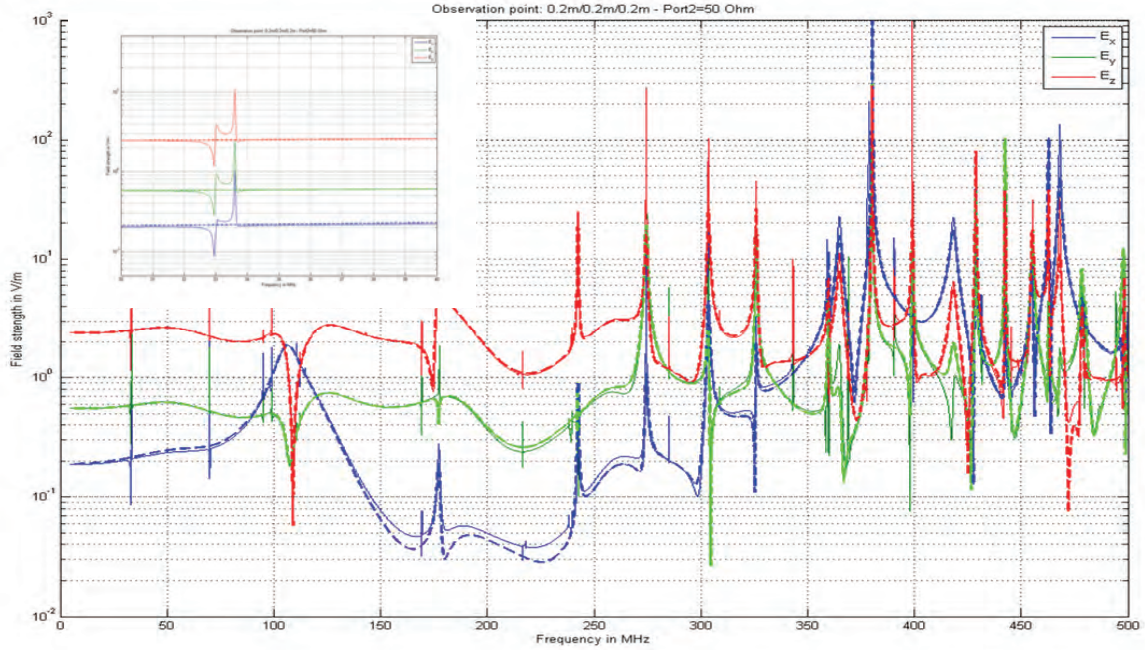


Figure 8: Electric field – comparison between *N*-port method and direct solution

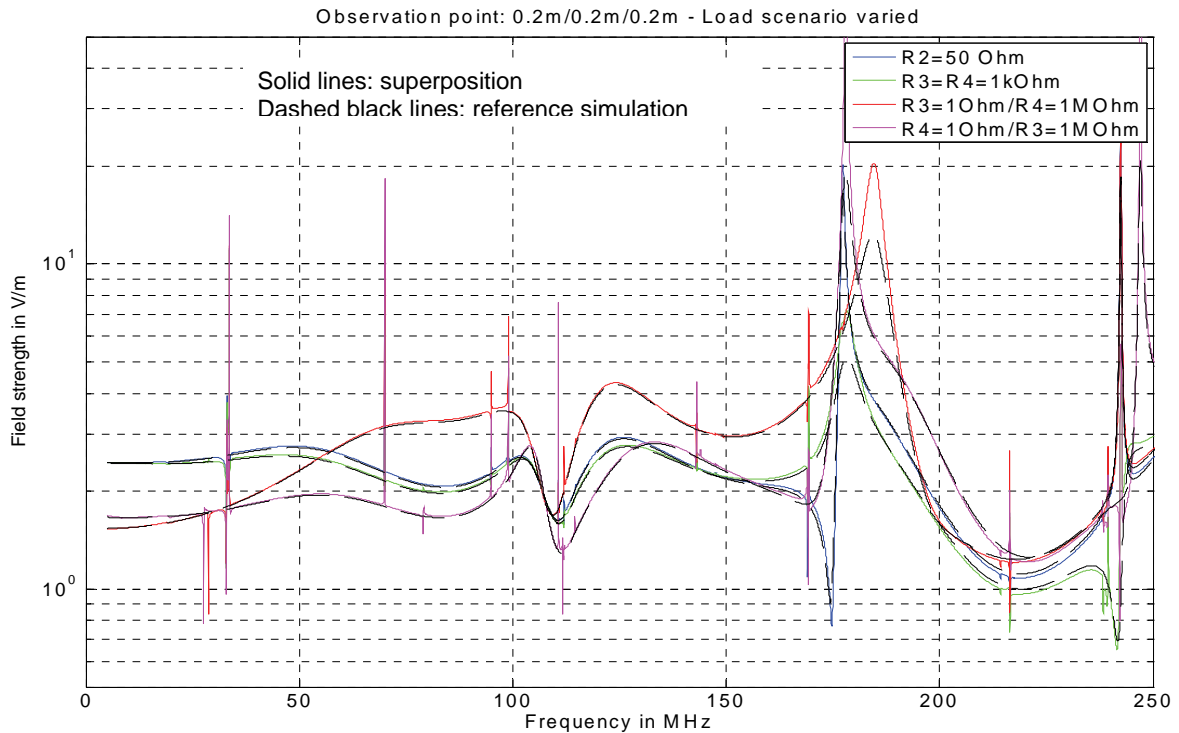


Figure 9: Load at ports 3 & 4 varied

During the initial field simulation the source port has been loaded with a small resistance of  $0.1\ \Omega$ , while the open ports have been loaded with resistors of  $1\ \text{M}\Omega$ . The small resistor value has been included for convenience; moving the excitation from one port to the other only requires changing loads, but not adding and removing loads; the

large resistors were necessary because the program can only calculate voltages across impedances [6]. The results can be improved, i.e. the false resonances be decreased, if better approximations for the short circuit and open ports are used. When replacing the  $0.1\ \Omega$  resistor with  $1\ \mu\Omega$  values and the  $1\ \text{M}\Omega$  resistors with  $1\ \text{G}\Omega$  the false

resonances almost disappear. These results are shown in Figure 10.

A reason for this behavior becomes obvious when scrutinizing the impedance matrix. Being a passive network the impedance matrix must be symmetric, i.e.  $Z_{ij}=Z_{ji}$  is required for each pair  $i$  and  $j$ . A closer look at two pairs in Figure 11 reveals that  $Z_{12}$  and  $Z_{21}$  as well as  $Z_{34}$  and  $Z_{43}$  are

generally identical, except for some sharp nulls which occur at slightly different frequencies. These nulls occur in systems with high Quality-factors. Their effect can be reduced by considering the finite conductivity of the cell walls and the septum. This would, however, result in more unknowns for the equation system and longer computation times. Alternatively a lossy dielectric ('lossy brick in Figure 7) can be placed inside the TEM wave guide

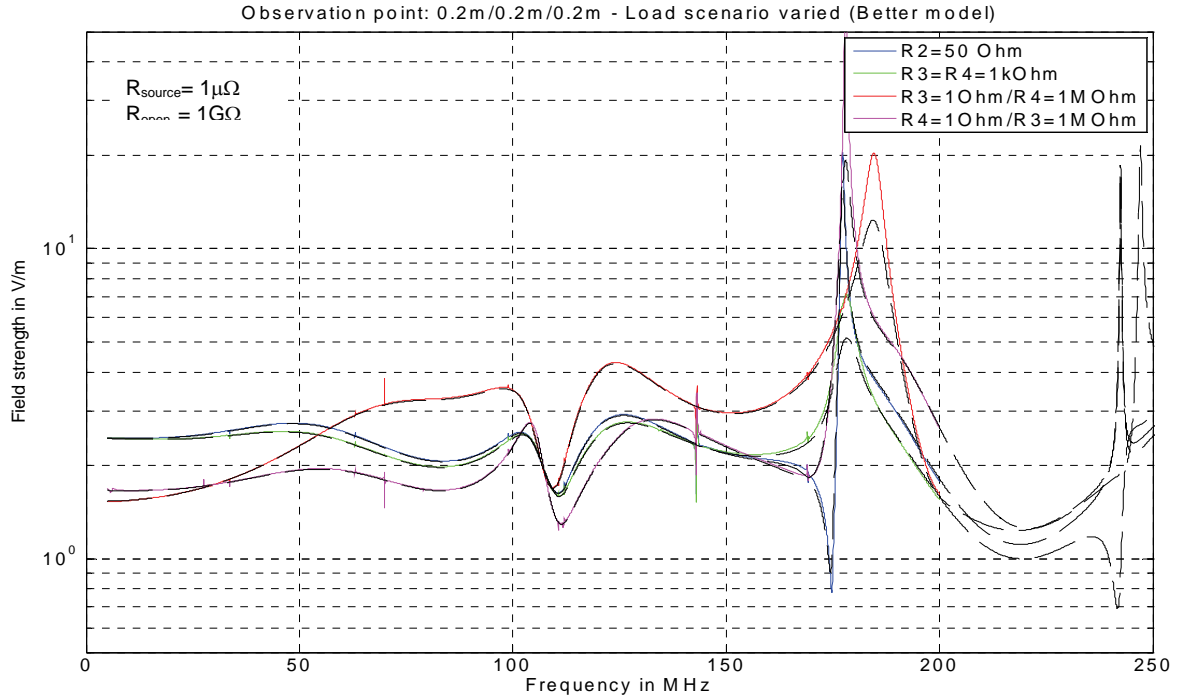


Figure 10: Load at ports 3 & 4 varied (better model)

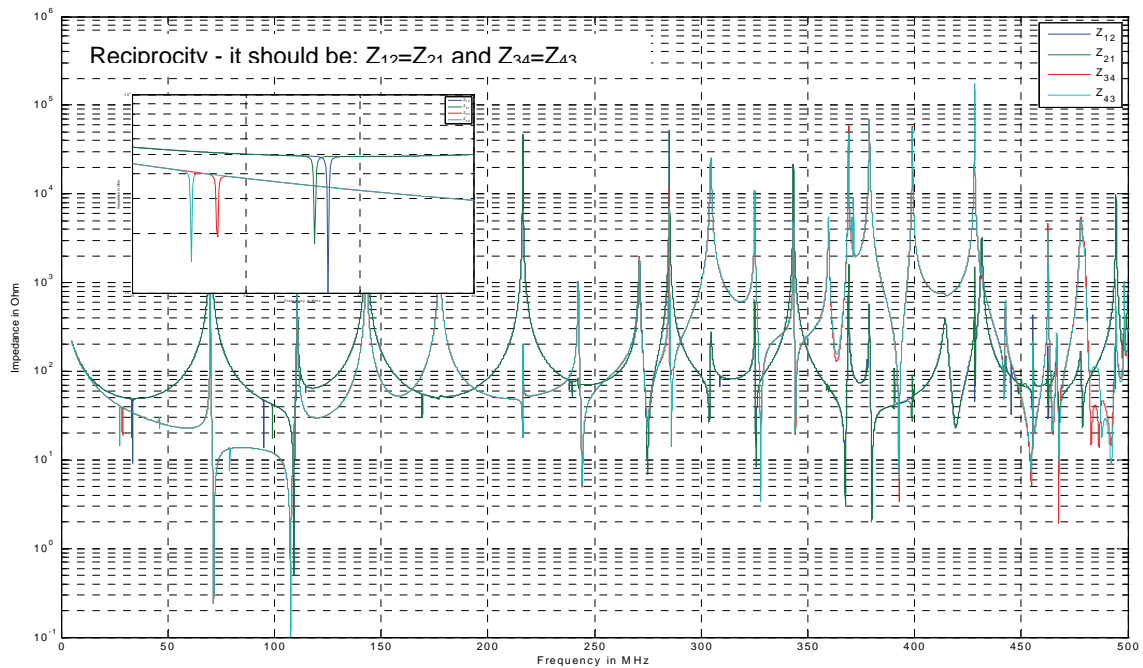


Figure 11: Symmetry of  $N$ -port impedance matrix



The use of this  $N$ -port method to compute field strengths requires  $N$  field simulations for a system with  $N$  accessible ports. It is therefore only of an advantage if at least  $N$  different termination scenarios are to be investigated. A possible application is illustrated again using the example of the TEM waveguide.

Figure 12 shows a number of observation points forming the working volume of the TEM waveguide. The model has a resonance around 80 MHz resulting in widely different field strength values at different observation points. The ratio between highest and lowest field strength, as can be seen from Figures 13 and 14, is about 5.

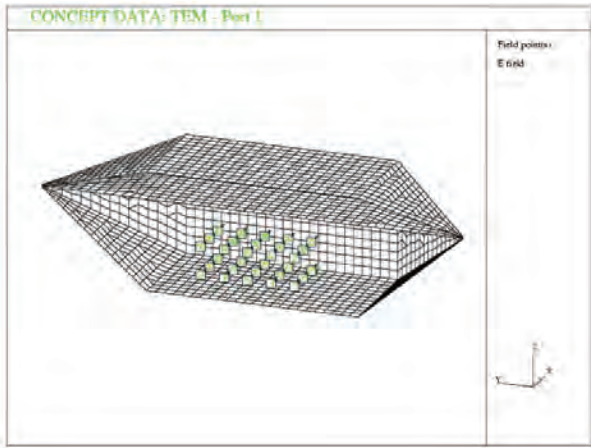


Figure 12: Field observation points

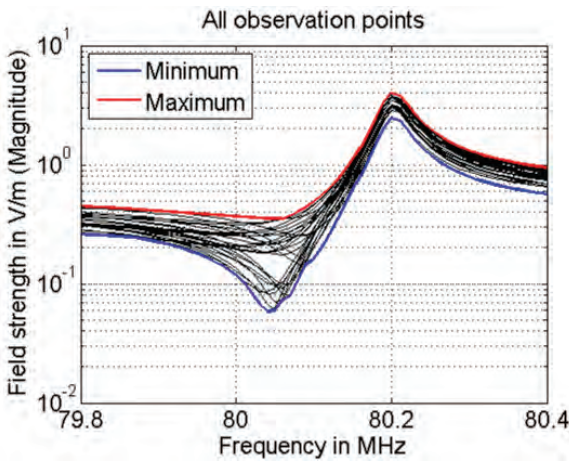


Figure 13: Field strength across the working volume

#### IV. CONCLUSION

Linear systems with distributed parameters or coupled antennas can be considered as  $N$ -port networks and field strength values can be updated for various termination scenarios without repeating full-wave field simulations.

The electric field around this frequency has a maximum value between septum and the upper part of the cell, at the location of port 3 (see Figure 15). Therefore loading port 3 can be expected to dampen this resonance. The results for 4 resistance values are added in Figure 14. When decreasing the resistance value the field uniformity just below 80 MHz improves, but the performance above 80 MHz gets worse. A resistance value around 1 k $\Omega$  seems to give the best results.

In Figure 16 the resistance value is now changed in small steps and the field uniformity is shown as color code depending on frequency and resistance value.

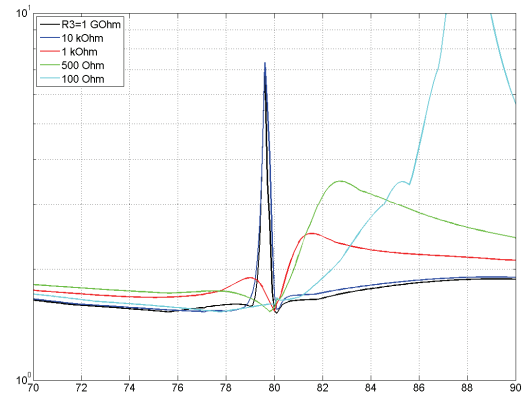


Figure 14: Field uniformity for a various load at port 3

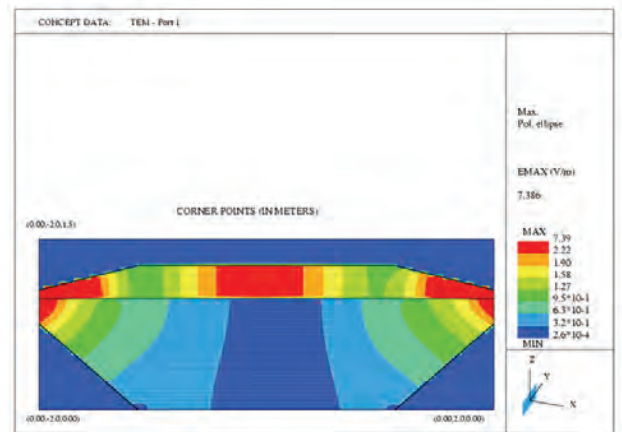


Figure 15: Field distribution around 80 MHz

The method can be applied as a post-processing routine after field simulations, and does not depend on the usage of specific field solvers. However, it is important that accurate  $N$ -port parameters are available. In particular if systems with high  $Q$ -factors, i.e. with sharp resonance are investigated the symmetry of the  $N$ -port matrices is essential.

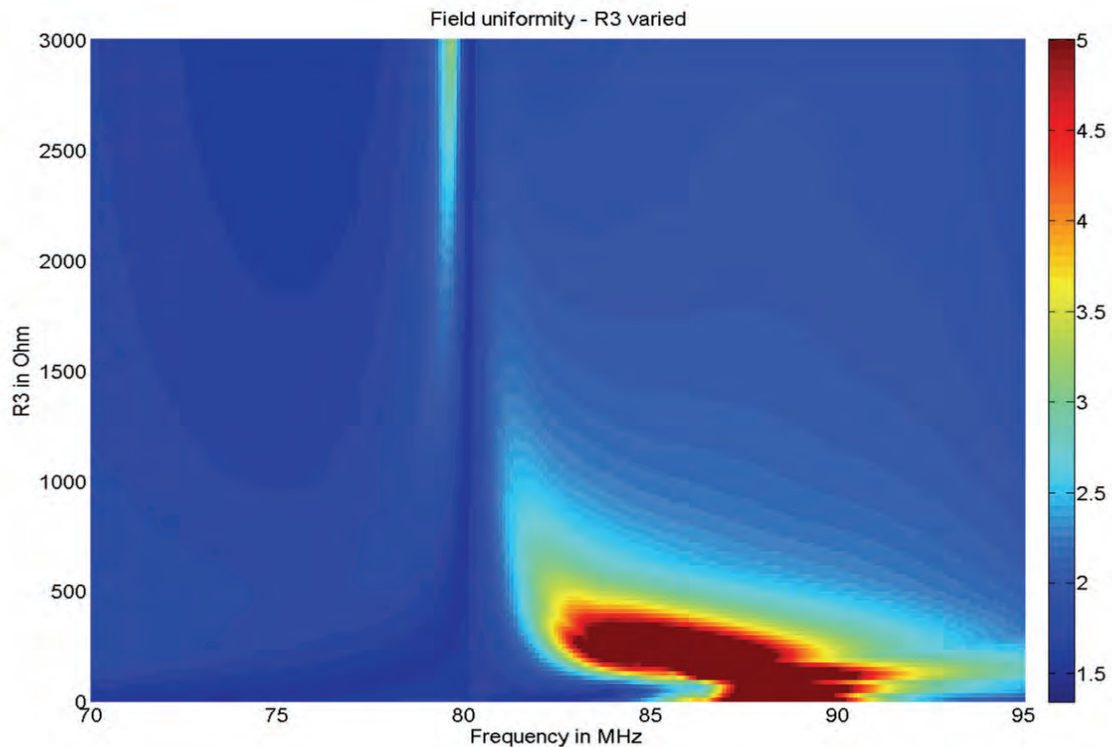


Figure 16: Field uniformity for a various load at port 3 (fine resistance steps)

#### REFERENCES

- [1] Chan, Chan, Chan: '*Analysis of Linear Networks and Systems*', Addison Wesley Publishing Company, Reading (Mass.), Menlo Park (Ca), London, Don Mills (Ontario), 1972
- [2] F. Schlagenhauser: '*Investigation of the Coupling between HF Antennas on Complex Structures*', IEEE EMC Symposium, Denver, 1998, pp 696-700
- [3] F. Schlagenhauser, J. He, K. Fynn: '*Using N-Port Models for the Analysis of Radiation Structures*', Proc. of IEEE Int. Symp. on EMC, Minneapolis, 2002, pp 297-302
- [4] F. Schlagenhauser, K. Fynn, A. Cantoni: '*Efficient Simulation of Radiated Emissions from PCBs for Varying Port Terminations*', Int. IEEE Symposium on EMC, 2003, Istanbul
- [5] Matlab home page: [www.mathworks.com](http://www.mathworks.com)
- [6] CONCEPT home page: [www.tu-harburg.de/~tebr](http://www.tu-harburg.de/~tebr)
- [7] P. Kay, F. Schlagenhauser: '*Application of Field Simulation to a Hybrid TEM Cell: New Tools for Old Systems*', EMC Wroclaw, June 2006
- [8] P. Kay, F. Schlagenhauser, H. Fan: '*Figures of Merit for a Hybrid TEM-Reverberation Chamber*', Int. Zurich-Symposium on EMC, Munich, 2007